THE JOURNAL OF PHYSICAL CHEMISTRY B

Article

pubs.acs.org/JPCB

Watson−Crick and Sugar-Edge Base Pairing of Cytosine in the Gas Phase: UV and Infrared Spectra of Cytosine·2-Pyridone

Jann A. Frey, Philipp Ottiger, and Samuel Leutwyler*

Department of Chemistry and Biochemistry, University of Bern, Freiestrasse 3, CH-3012 Bern, Switzerland

Supporting Information

ABSTRACT: While keto-amino cytosine is the dominant species in aqueous solution, spectroscopic studies in molecular beams and in noble gas matrices show that other cytosine tautomers prevail in apolar environments. Each of these offers two or three H-bonding sites (Watson−Crick, wobble, sugar-edge). The mass- and isomer-specific $S_1 \leftarrow S_0$ vibronic spectra of cytosine·2-pyridone (Cyt·2PY) and 1-methylcytosine·2PY are measured using UV laser resonant two-photon ionization (R2PI), UV/UV depletion, and IR depletion spectroscopy. The UV spectra of the Watson−Crick and sugar-edge isomers of Cyt·2PY are separated using UV/UV spectral hole-burning. Five different isomers of Cyt·2PY are observed in a supersonic beam. We show that the Watson−Crick and sugar-edge dimers of keto-amino cytosine with 2PY are the most abundant in the beam, although keto-amino-cytosine is only the third most abundant tautomer in the gas phase. We identify the different isomers by combining three different diagnostic tools: (1) methylation of the cytosine N1−H group prevents formation of both the sugar-edge and wobble isomers and gives the Watson−Crick isomer exclusively. (2) The calculated ground state binding and dissociation energies, relative gas-phase abundances, excitation and the ionization energies are in agreement with the assignment of the dominant Cyt·2PY isomers to the Watson−Crick and sugar-edge complexes of keto-amino cytosine. (3) The comparison of calculated ground state vibrational frequencies to the experimental IR spectra in the carbonyl stretch and NH/OH/CH stretch ranges strengthen this identification.

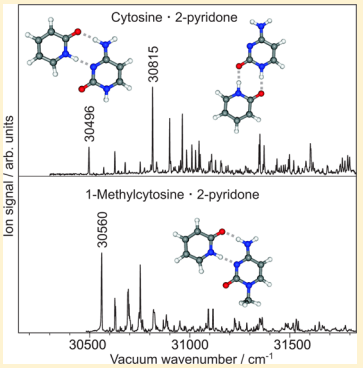

1. INTRODUCTION

The nucleobase cytosine exists in a large number of tautomeric forms, some of which exhibit two rotamers, denoted 2a/b and 3a/b in Figure 1. The relative stability of the cytosine tautomers/rotamers depends on the temperature and the chemical environment. The biologically relevant N1−H or keto-amino tautomer **1** is by far the most abundant in aqueous solution.[1] In 1988, Szczezniak et al. found that the hydroxy-amino tautomers **2a** and **2b** (see Figure 1) dominate the IR spectra in inert gas matrices.[2,3] A year later, Brown et al. reported the supersonic-jet millimeter-wave absorption spectra of three species to which they assigned the keto-amino **1**, enol-amino **2b**, and keto-amino **3a** or **3b** tautomers.[4] Very recently, Alonso et al. have identified the five tautomers shown in Figure 1, based on the analysis of the ^{14}N hyperfine structure in the molecular-beam Fourier-transform microwave spectra.[5] The relative gas-phase concentrations of different cytosine tautomers have been determined also by X-ray photoemission spectroscopy.[6,7] Kostko et al.[8] have studied the photoionization curves of cytosine using single-photon vacuum-ultraviolet (VUV) photoionization in combination with electronic structure calculations.[8] De Vries and co-workers have performed pioneering UV and infrared spectroscopic measurements of cytosine cooled in a supersonic jet.[9,10] Using spectral hole-burning, they identified three species: the keto-amino tautomer **1**, the hydroxy-amino tautomer **2a**/**2b**, and a third tautomer that remained unassigned.[9,10] More recently, Lobsiger et al. have determined the tautomer-specific ionization potential of keto-amino cytosine[11] and analyzed the UV spectrum of keto-amino **1** tautomer in detail.[12] Theoretical gas-phase calculations for experimentally relevant temperatures[13,14] have confirmed that the tautomers **1**, **2a**, and **2b** account for close to 95% of the gas-phase tautomer distribution.

Each of the five main rotamers/conformers offers several double H-bonding sites, which are denoted by Watson−Crick (WC), wobble (W), and sugar-edge (S), as marked in Figure 1. Upon H-bonding to a second nucleobase, each tautomer can form dimers with up to three different H-bonding patterns, giving rise to more than a dozen tautomer/H-bond isomers. In this work, we investigated jet-cooled dimers of cytosine with 2-pyridone (Cyt·2PY) by mass-specific ultraviolet (UV) and infrared/UV double resonance spectroscopies. Like uracil and thymine, 2-pyridone can form two H-bonds via a cis-amide group. Unlike uracil and thymine, 2PY presents only one cis-amide function, which dramatically reduces the number of possible dimers formed with other nucleobases. Furthermore, 2PY is a UV chromophore whose $S_1(\pi\pi^*)$ state exhibits a fluorescence lifetime of $\tau_{fl} = 9 \pm 1$ ns,[15] which allows both efficient excitation/ionization and high-resolution UV spectroscopy.[15] We have previously employed 2PY to probe the

Received: September 27, 2013
Revised: November 22, 2013
Published: January 2, 2014

   dx.doi.org/10.1021/jp409660b | J. Phys. Chem. B 2014, 118, 682−691

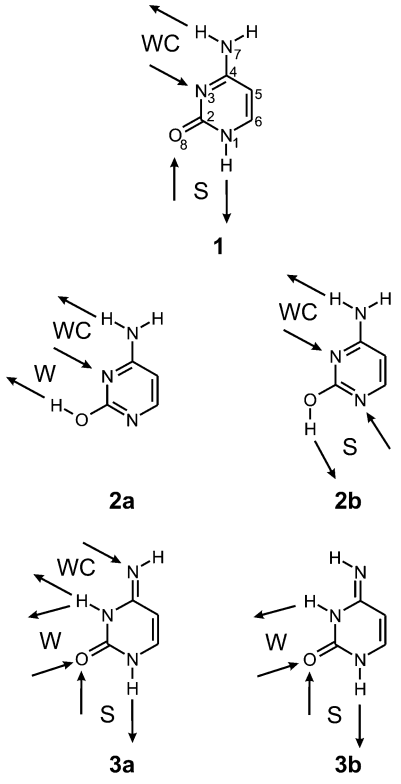

Figure 1. The cytosine tautomers/rotamers **1**, **2a**, **2b**, **3a**, and **3b** considered in this work (tautomer numbering according to ref 3). The arrows indicate the double hydrogen-bonding sites, denoted Watson–Crick (WC), sugar-edge (S), and wobble (W).

properties of antiparallel double H-bonds formed with 2-aminopyridine,[16] with fluorobenzenes,[17] with uracil, fluorouracil, thymine, and other methyluracils,[18,19] and with 9-methyladenine.[20]

The dimer of keto-amino Cyt with 2PY can be viewed as a model of the Cyt:uracil mismatch base pair, which has been observed in crystal structures of RNAs and RNA duplexes.[21,22] The first observation of the Cyt:uracil base pair was in the RNA dodecamer duplex $(r\text{-}GGACUUCGGUCC)_2$, where the four non-complementary nucleotides in the middle of the sequence do not form a loop but a highly regular double helix.[21]

The goals of this work are (1) to spectroscopically identify the dimers that are formed with the different possible cytosine tautomers in the cold and solvent-free supersonic jet environment, (2) to check the assignment by chemical substitution of cytosine, (3) to quantify the H-bond interaction strengths via the intermolecular vibrational frequencies and by the changes of the intramolecular N—H, OH, and C=O vibrational frequencies. In this way, we provide a quantitative spectroscopic basis for investigating the H-bonds in these model nucleobase dimers.

For the related cytosine dimer, de Vries and co-workers have identified a single H-bond isomer consisting of two cytosine **1** tautomers, revealed by IR/UV double resonance experiments.[9,10,23] In the H-bonded cytosine–guanine complex, the amino-keto **1** and enol-amino **2a**/**b** isomers of cytosine have been identified.[23−25] Brutschy and co-workers have investigated the IR spectra of the jet-cooled dimers 4-aminopyrimidine-1-methylthymine and 4-aminopyrimidine-6-methyl-4-pyrimidinone as mimics of the adenine–thymine (A–T) Watson–Crick (WC) base pair.[26]

Since only the five cytosine tautomers shown in Figure 1 have been observed in the gas phase,[4−8,27] we will restrict the discussion to these forms. Each conformer offers two to three double hydrogen binding sites, totaling 11 binding sites. For a definitive clarification of the H-bonding patterns observed, we have also studied the 1-methylcytosine·2-pyridone complex (1MCyt·2PY). In 1MCyt, the keto ↔ enol tautomerism is suppressed and the biologically irrelevant sugar-edge binding site is blocked, which allows one to unambiguously assign the observed 1MCyt·2PY isomer, as discussed below in detail. Note that 2PY also exists as the 2-hydroxypyridine (2HP) tautomer in the molecular beam, but the longest-wavelength absorption of 2HP is at 277 nm, far outside the 305–330 nm region investigated in this work. Therefore, all the UV and IR/UV spectra reported here arise from complexes involving the 2PY tautomer.

2. EXPERIMENTAL AND COMPUTATIONAL METHODS

2.1. Experimental Techniques. The Cyt·2PY and 1MCyt·2PY complexes were produced and cooled in a pulsed supersonic Ne jet at backing pressures of 1–1.5 bar. The 20 Hz pulsed nozzle was heated to 240 °C for the cytosine experiments and to 220 °C with 1-methylcytosine. A 1:1 mixture of cytosine (or 1-methylcytosine) and 2-pyridone was placed in the sample holder, and 2-pyridone was replenished by flowing the Ne through a 2PY reservoir heated to 100 °C.

In the two-color resonant two-photon ionization (2C-R2PI) experiments, excitation was performed with the frequency doubled output (~100 μJ) of a Lambda Physik FL3002 dye laser pumped by a Innolas Spitlight 600 Nd:YAG. Ionization was performed with ~800 μJ of 266 nm from the same pump laser or 228 nm produced by an Ekspla UV-OPO system. For the UV/UV depletion experiments, the Lambda-Physik dye laser was used to deplete the 2C-R2PI signal, which was produced with the UV output from a Radiant Dyes NarrowScan dye laser (excitation, 200 μJ/pulse) and ionization at 266 or 228 nm (600 μJ/pulse).

The IR/UV depletion spectroscopy is based on the two-color R2PI setup. The excitation pulse energy was increased to ~350 μJ to achieve partial optical saturation of the 2-pyridone $S_1 \leftarrow S_0$ transition, resulting in a larger and more stable signal. The IR light in the 2600–4000 cm^{-1} range (~7 mJ) was generated using a LaserVision OPO/OPA system[28] operating at 10 Hz that was pumped by an injection-seeded Continuum PL8000 Nd:YAG laser. The IR beam, which precedes every second shot of the UV lasers by 100 ns, was arranged nearly collinearly to the two UV beams and was mildly focused using an f = 1000 mm CaF_2 lens. An additional $AgGaSe_2$ crystal was used to produce ~0.8 mJ of IR in the 1400–2000 cm^{-1} C=O stretch region. For these experiments, the IR laser was arranged anticollinearly and focused with an f = 500 mm CaF_2 lens.

2.2. Computational Methods. The geometries of 2-pyridone, cytosine, and 1-methylcytosine and of the 12 possible H-bonded dimers were optimized with the resolution-of-the-identity (RI) second-order Møller–Plesset (MP2) frozen-core method using the aug-cc-pVTZ basis set. On the basis of these geometries, the dimer binding energies were extrapolated using the aug-cc-pVXZ (X = 2, 3, 4) series of basis sets and Dunning's exponential extrapolation scheme.[29] The additional correlation energy contributions were evaluated at the CCSD(T) level with a modified aug-cc-pVDZ basis set (aVDZ′) where the most diffuse d functions of the C, N, and O atoms were removed. For H-bonded dimers, such a procedure has been shown to yield

dx.doi.org/10.1021/jp409660b | J. Phys. Chem. B 2014, 118, 682–691

Table 1. Calculated Binding Energies D_e and Dissociation Energies D_0 of the Cytosine·2-Pyridone Isomers (in kcal/mol)

complex	isomer	D_e(MP2/CBS)[a]	ΔCCSD(T)/aVDZ′ [b]	D_e	ΔZPE[c]	D_0
Cyt**1**·2PY	Watson−Crick	−22.80	+0.47	−22.33	+1.40	−20.93
Cyt**1**·2PY	sugar-edge	−23.04	+0.59	−22.45	+1.17	−21.28
Cyt**2a**·2PY	wobble	−17.01	+0.48	−16.53	+1.02	−15.51
Cyt**2a**·2PY	Watson−Crick	−15.54	+0.42	−15.12	+0.97	−14.15
Cyt**2b**·2PY	Watson−Crick	−20.13	+0.47	−19.66	+1.21	−18.45
Cyt**2b**·2PY	sugar-edge	−18.86	+0.64	−18.22	+0.90	−17.32
Cyt**3a**·2PY	Watson−Crick	−17.53	+0.88	−16.65	+1.01	−15.64
Cyt**3a**·2PY	wobble	−15.51	+0.07	−15.44	+0.99	−14.45
Cyt**3a**·2PY	sugar-edge	−20.96	+0.31	−20.65	+1.28	−19.37
Cyt**3b**·2PY	wobble	−19.53	+0.31	−19.22	+1.27	−17.95
Cyt**3b**·2PY	sugar-edge	−20.50	+0.17	−20.33	+1.26	−19.07
1MCyt·2PY	Watson−Crick	−22.69	+0.42	−22.27	+1.31	−20.96

[a]MP2 complete basis set extrapolation using the aug-cc-pVXZ (X = 2, 3, 4) basis sets at the MP2/aVTZ geometries. [b]D_e(CCSD(T)/aug-cc-pVDZ′) − D_e(MP2/aug-cc-pVDZ′). [c]Zero point vibrational energy difference calculated at the MP2/aug-cc-pVDZ level.

binding energies D_e that are accurate to within 0.4 kcal/mol.[30] Harmonic vibrational frequencies and zero point energy corrections were calculated at the MP2/aug-cc-pVDZ level.

The gas-phase equilibrium constants for the formation of the different cytosine tautomers and of the Cyt·2PY and 1MCyt·2PY complexes were calculated with the *freeh* script of Turbomole 6.0,[31] using the MP2/aug-cc-pVTZ moments of inertia, the MP2/aug-cc-pVTZ + ΔCCSD(T)/aug-cc-pVDZ′ relative electronic energies, and the MP2/aug-cc-pVDZ vibrational frequencies. For the assignment of the excited state vibrational frequencies, the S_1 state normal modes of the Cyt·2PY and 1MCyt·2PY complexes were calculated at the CIS/6-31G(d,p) level. Vertical excitations were calculated at the CC2/aug-cc-pVDZ level on the MP2/aug-cc-pVTZ geometries. The adiabatic ionization energies and cation structures of the H-bonded dimers were calculated at the UB3LYP/6-311++G(d,p) level of theory.

For the interpretation of the infrared spectra, normal modes were calculated using the PW91 density functional method with the 6-311++G(d,p) basis set. The choice of this method/basis set combination was based on its good performance when compared to the measured IR spectra of the jet-cooled 2-aminopyridine·2-pyridone[16] and (2-aminopyridine)$_2$ dimers.[32]

The MP2 and CC2 calculations were performed with the TURBOMOLE 6.0 program package,[31] and Gaussian 03[33] was used for the CIS, DFT, and CCSD(T) calculations.

3. RESULTS AND DISCUSSION

3.1. Energetics and Thermodynamics. The binding energies D_e and dissociation energies D_0 of the Cyt·2PY or 1MCyt·2PY complexes are given in Table 1. The most stable Cyt·2PY complex is formed with the keto-amino **1** tautomer via the sugar-edge H-bonding site, with a calculated D_0 = −21.3 kcal/mol. The biologically relevant Watson−Crick dimer is slightly less stable with D_0 = −20.9 kcal/mol. The corresponding Watson−Crick dimer with 1-methylcytosine has a nearly identical dissociation energy of D_0 = −21.0 kcal/mol. Thus, methylation has little influence on the double H-bonds. The dissociation energies of the other nine dimers in Table 1 are more than 1.5 kcal/mol smaller than those of these three dimers. We thus expect their concentration in the supersonic jet to be considerably lower than those formed with the keto-amino **1** tautomer.

We then calculated the relative gas-phase abundances of the 5 Cyt tautomers and of the 12 H-bonded complexes over the range T = 1−600 K using gas-phase statistical thermodynamics and the rigid-rotor/harmonic-oscillator approximation. The cytosine tautomerization equilibria are shown in Figure 2a: The tautomer **2b** is the most stable species over the entire temperature range. The **1**:**2b**:**2a**:**3a** mole fractions are 0.12:0.64:0.21:0.03 at 298 K, in reasonable agreement with the 0.21:0.60:0.18:0.01 ratio calculated by Trygubenko et al.,[14] which was later experimentally confirmed by Schirmer and co-workers.[6,7] By fitting the infrared and UV spectra of cytosine tautomers in Ar matrices, Baszó et al.[3] found relative abundances of 0.22:0.44:0.26:0.08 at 450 K which are in excellent agreement with our calculated fractions of 0.20:0.48:0.24:0.07 at T = 450 K.

Figure 2b shows the calculated abundances of the Cyt·2PY complexes, which were scaled by the relative abundances of the corresponding Cyt tautomers. This scaling leads to a significant change in the relative abundances and the order of the minor isomers. Over the T = 1−600 K range, the combined abundances of the sugar-edge and Watson−Crick forms of Cyt**1**·2PY amount to ∼90% of all the dimers. Thus, although the amino-hydroxy tautomers **2a** and **2b** contribute the major gas-phase fraction of the monomers as seen in Figure 2a, they play a relatively minor role for the complexes, because their binding and dissociation energies are considerably smaller than those of the keto-amino tautomer **1**. Figure 2b predicts that the main isomers are those of Cyt**1**·2PY, with a sugar-edge/Watson−Crick ratio that is about 1.5:1 at the temperature of our nozzle (490−510 K).

Due to the rapid dilution and vibrational cooling in the early stages of the supersonic jet, we expect the interconversion between different tautomers to be halted early within the expansion. On the basis of the experimental data discussed below, one can estimate that the relative abundance of the Cyt tautomers freezes in at an effective temperature of 400 ± 40 K. On the other hand, the interconversion of different H-bonded isomers may continue to lower temperatures, because of the much lower barriers separating the different H-bond isomers.

3.2. Resonant Two-Photon Ionization and UV/UV Hole-Burning Spectroscopy. *3.2.1. Ionization at 266 nm.* Figure 4 presents the 2C-R2PI spectra of Cyt·2PY and 1MCyt·2PY over the 30500−32500 cm^{-1} range with ionization at 266 nm. Since 1-methylcytosine cannot form the enol-amino tautomers **2a**/**2b**, only the keto-amino form is abundant in the molecular beam, with the imino-hydroxy tautomers being far less stable. Correspondingly, the 1MCyt·2PY spectrum in

dx.doi.org/10.1021/jp409660b | J. Phys. Chem. B 2014, 118, 682−691

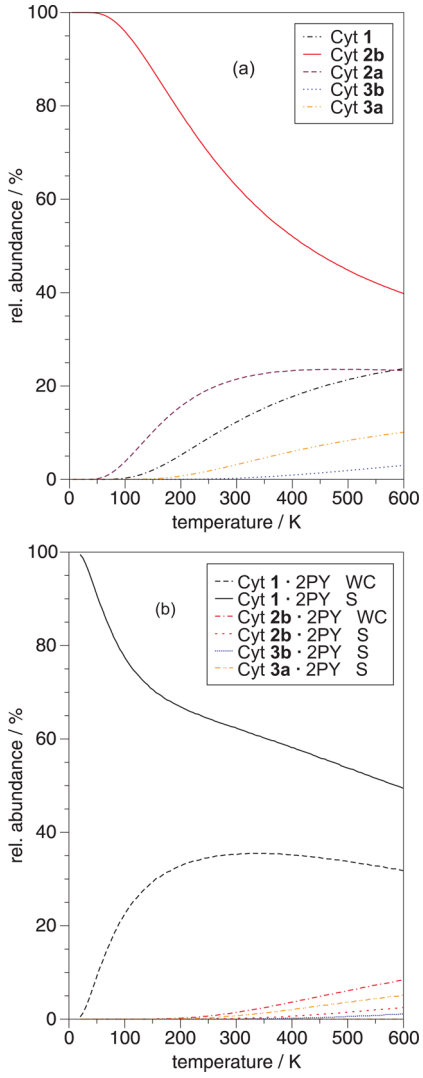

Figure 2. (a) Calculated relative abundances of the cytosine (Cyt) tautomers/rotamers (see Figure 1) over the temperature range T = 1–600 K. (b) Calculated relative abundances of the six most stable cytosine·2-pyridone (2PY) complexes. See Figure 1 for the tautomer nomenclature.

Figure 4b is assigned to the Watson–Crick complex (see Figure 3).

Using UV/UV hole-burning, we find that the Cyt·2PY spectrum in Figure 4a includes contributions from two isomers: The spectrum of the minor isomer *A* with a relative intensity of

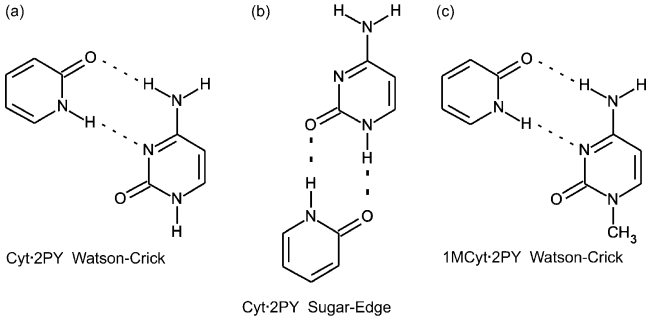

Figure 3. Schematic structures of the two cytosine·2-pyridone and the 1-methylcytosine·2-pyridone complexes identified experimentally.

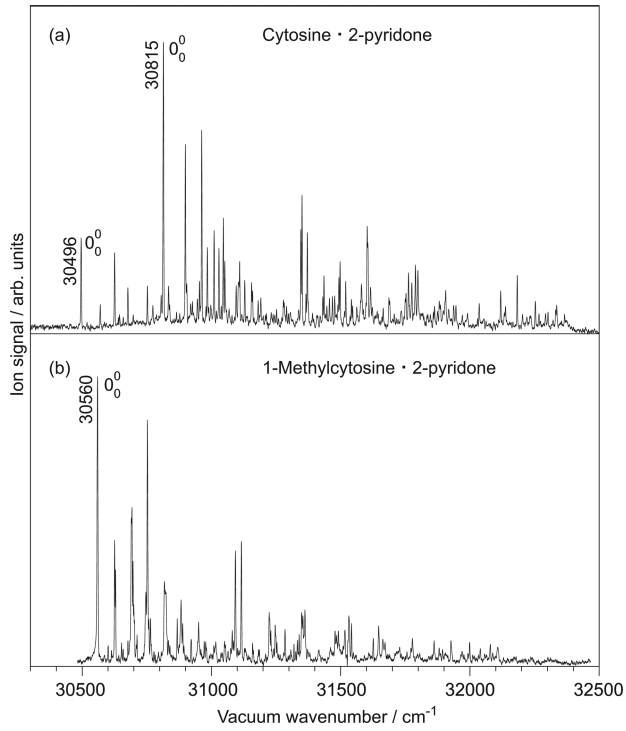

Figure 4. Two-color resonant two-photon ionization spectra of (a) cytosine·2-pyridone (isomers *A* and *B*, see the text) and (b) of 1-methylcytosine·2-pyridone.

30% exhibits a strong electronic origin at 30496 cm^{-1}, as shown in Figure 5c. As seen in Figure 5b, the major isomer *B* exhibits an electronic origin at 30815 cm^{-1}. Together, these spectra sum up to the total observed Cyt·2PY spectrum in Figure 5a. The peak positions and assignments of both Cyt·2PY isomers and of 1MCyt·2PY are indicated in Figure 5 and summarized in Table 3. The corresponding CIS/6-31G(d,p) normal-mode frequencies are given in Table 4.

The first two strong bands in the spectrum of the minor isomer *A* seen in Figure 5c are identified as the in-plane intermolecular opening mode ω' at 74 cm^{-1} and the stretching mode σ' at 130 cm^{-1}. Combinations and overtones of these two vibrations are identified as $2\omega'$ at 148 cm^{-1}, $\omega' + \sigma'$ at 202 cm^{-1}, $2\sigma'$ at 256 cm^{-1}, and $3\sigma'$ at 382 cm^{-1}. The other vibronic bands are assigned to intramolecular vibronic transitions of the 2PY moiety.[34] The first overtone of the 2PY out-of-plane twist/bend mode, $2\nu'_1$, is identified at 181 cm^{-1}. Three medium intense bands appear at 534, 556, and 789 cm^{-1}. These have been observed in other dimers of 2PY[19] and are assigned accordingly to the in-plane modes ν'_5, ν'_6, and ν'_{10} of 2-pyridone. At 664 cm^{-1}, the combination band $\nu'_5 + \sigma'$ is identified.

As seen in Figure 5b, the major isomer *B* exhibits intermolecular vibronic transitions in the opening (ω') mode at 85 cm^{-1} and the stretching σ' vibration at 149 cm^{-1}. Combinations and overtones of these in-plane vibrations appear at 170 cm^{-1}, $2\omega'$, 232 cm^{-1}, $\omega' + \sigma'$, 296 cm^{-1}, $2\sigma'$, 316 cm^{-1}, $2\omega' + \sigma'$, and 377 cm^{-1}, $2\sigma' + \omega'$. Again, two intramolecular vibrations of 2PY are identified, ν'_5 at 534 cm^{-1} and ν'_6 at 558 cm^{-1}; see also Table 3.

The intermolecular vibrations also dominate the low-frequency region of the spectrum of 1MCyt·2PY shown in Figure 5c. The in-plane opening ω', shear χ', and stretch σ' excitations are observed at 66, 93, and 131 cm^{-1}. A large number of overtone and combination bands can be identified;

dx.doi.org/10.1021/jp409660b | J. Phys. Chem. B 2014, 118, 682–691

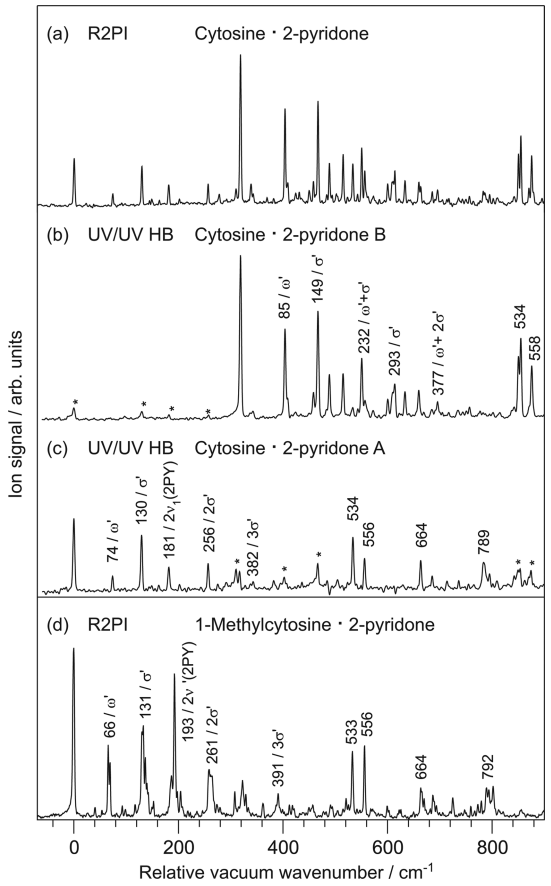

Figure 5. Two-color R2PI spectra of (a) cytosine·2-pyridone and (d) 1-methylcytosine·2-pyridone with ionization at 266 nm, in the region of the intermolecular vibrations. (b, c) Isomer-specific cytosine·2-pyridone spectra, separated by UV hole-burning at the origins of isomer *A* at 30496 cm^{-1} and of isomer *B* at 30815 cm^{-1}. Residual signals of isomer *A* in part b and of isomer *B* in part c are marked by asterisks. The respective 0_0^0 bands of isomer *A* and 1MCyt·2PY are aligned for comparison.

see Table 3. The 2PY intramolecular excitations $2\nu'_1$, ν'_5, and ν'_{10} are observed at 193, 533, and 792 cm^{-1}. Combinations with intermolecular vibrations are also quite prominent, e.g., $2\nu'_1 + \omega'$ at 258 cm^{-1} and $2\nu'_1 + \sigma'$ at 323 cm^{-1}.

The calculated frequencies of all cytosine·2-pyridone species and of 1-methylcytosine·2-pyridone are collected in Table 4. For the unambiguously identified 1MCyt·2PY complex, the calculated and experimental frequencies agree within ∼10%. This is typical for the CIS calculated intermolecular vibrations of dimers with doubly H-bonded 2PY.[17−20,35,36] The observed opening ω' and stretch σ' frequencies show only little variation between the different dimers. The intermolecular vibration frequencies alone do not allow the observed isomers to be identified unambiguously.

3.2.2. Ionization at 228 nm. We then measured UV/UV depletion spectra of Cyt·2PY using ionization at 228 nm, which are shown in Figure 6. Besides the UV band systems of the isomers discussed above, additional bands appear. We can attribute these to three additional Cyt·2PY isomers using UV/UV depletion measurements, as shown in Figure 6d−f. The corresponding signal intensities are weak and the S/N ratio is too low to be used for a thorough interpretation and assignment of vibrational bands. We note, however, that the distribution of two major and several minor isomers is in good agreement with the calculated relative abundances of the Cyt·2PY complexes shown in Figure 2 and discussed above.

The two isomers observed with ionization at 266 nm obviously have a significantly lower ionization energy than that of the isomers which are observed only with ionization at 228 nm. We have calculated the adiabatic ionization energies of all 12 dimers using the UB3LYP method and the 6-311++G(d,p) basis set. The results are shown in Table 2. The calculated adiabatic ionization energies (AIE) indeed show a remarkable spread of values, between AIE = 7.01 eV for the Watson−Crick isomer of Cyt**3a**·2PY and AIE = 7.90 eV for the wobble isomer of Cyt**2a**·2PY. We do not claim high accuracy for these values but note that the adiabatic ionization energies of cytosine dimers calculated by Kostko et al.[8] also lie in the range IE = 7.31−7.64 eV.

According to the calculations, the Cyt**3a**·2PY isomer with the lowest ionization energy should appear in the jet at very low concentration (<0.1%), which explains why we do not observe it. The isomers with the next higher AIEs are precisely the Cyt**1**·2PY sugar-edge and Watson−Crick isomers that are formed with the highest abundance. Their ionization energies of these two species lie close together at AIE = 7.41 and 7.43 eV, while the other isomers have 0.2−0.4 eV higher ionization

Table 2. CC2/aug-cc-pVDZ Calculated Vertical Excitation Energies (in cm^{-1}) and Oscillator Strengths *f* (in the Length Representation) of the $S_1 \leftarrow S_0$ and $S_2 \leftarrow S_0$ Excitations of the Cytosine·2-Pyridone Isomers, Calculated at the MP2/aug-cc-pVTZ Geometries[a]

complex	isomer	S_1	$f(S_1 \leftarrow S_0)$	S_2	$f(S_2 \leftarrow S_0)$	ionization energy
Cyt**1**·2PY	Watson−Crick	**34841**	0.070	39178	0.055	**7.43**
Cyt**1**·2PY	sugar-edge	**35149**	0.071	38447	0.091	**7.41**
Cyt**2a**·2PY	wobble	35116	0.078	38899	0.099	7.90
Cyt**2a**·2PY	Watson−Crick	35007	0.071	38860	0.122	7.86
Cyt**2b**·2PY	Watson−Crick	34907	0.067	39209	0.118	7.67
Cyt**2b**·2PY	sugar-edge	35113	0.087	40126	0.128	7.80
Cyt**3a**·2PY	Watson−Crick	34817	0.066	40951	0.222	7.01
Cyt**3a**·2PY	wobble	35004	0.075	40689	0.121	7.63
Cyt**3a**·2PY	sugar-edge	35357	0.086	40111	0.240	7.75
Cyt**3b**·2PY	wobble	35258	0.077	41187	0.117	7.78
Cyt**3b**·2PY	sugar-edge	35350	0.085	40643	0.247	7.73
1MCyt·2PY	Watson−Crick	**34803**	0.067	38352	0.114	**7.08**

[a]The adiabatic ionization energies (in eV) are calculated at the UB3LYP/6-311++G(d,p) level.

dx.doi.org/10.1021/jp409660b | J. Phys. Chem. B 2014, 118, 682−691

Table 3. Experimental S_1 Vibrational Frequencies (in cm^{-1}) of the Cytosine·2-Pyridone Dimers *A* (Watson−Crick) and *B* (Sugar-Edge) and of the 1-Methylcytosine·2-Pyridone Watson−Crick Dimer

	cytosine·2-pyridone		1-methylcytosine·2-pyridone
vibronic transition	Watson−Crick	sugar-edge	Watson−Crick
0_0^0 band	(30 496)	(30 815)	(30 560)
β'		22	27
θ'			41
δ'			54
ω'	74	85	66
$\beta' + \omega'$			70
χ'			93
$\theta' + \delta'$			97
σ'	130	149	131
$2\omega'$	148	170	133
$2\nu_1'$(2PY)	181	197	193
$\omega' + \sigma'$	202	232	
$2\nu_1'$(2PY) + ω'		281	258
$2\sigma'$	256	296	263
$2\omega' + \sigma'$		316	264
$2\nu_1'$(2PY) + σ'		341	323
$3\sigma'$	382		391
$2\sigma' + \omega'$		377	329
ν_5'(2PY)	534	534	533
ν_6'(2PY)	556	558	556
ν_5'(2PY) + σ'	664		
ν_{10}'(2PY)	789		

Table 4. Calculated CIS/6-31G(d,p) Normal Mode Frequencies (in cm^{-1}) of 11 Dimers of Cytosine·2-Pyridone and the Watson−Crick Isomer of 1-Methylcytosine·2-Pyridone

complex	isomer	β'	θ'	δ'	ω'	χ'	σ'
Cyt**1**·2PY	Watson−Crick	25.6	43.2	58.2	75.0	90.6	122.9
Cyt**1**·2PY	sugar-edge	17.3	46.3	73.0	80.1	93.0	133.1
Cyt**2a**·2PY	wobble	33.9	27.6	75.5	60.0	92.2	127.1
Cyt**2a**·2PY	Watson−Crick	25.5	23.8	63.8	51.9	86.9	121.8
Cyt**2b**·2PY	Watson−Crick	31.7	17.1	76.0	70.3	111.0	121.1
Cyt**2b**·2PY	sugar-edge	23.8	33.5	56.5	69.3	90.6	119.6
Cyt**3a**·2PY	Watson−Crick	17.3	27.8	75.8	71.0	89.9	128.4
Cyt**3a**·2PY	wobble	17.7	33.9	56.6	67.7	83.8	119.7
Cyt**3a**·2PY	sugar-edge	18.8	42.9	58.7	78.8	89.5	128.0
Cyt**3b**·2PY	wobble	18.8	42.8	80.2	70.3	87.2	128.3
Cyt**3b**·2PY	sugar-edge	18.8	42.3	59.4	77.0	89.0	126.7
1MCyt·2PY	Watson−Crick	24.7	39.2	55.2	68.2	89.8	121.1

energies. The AIE calculations therefore confirm that the two observed species *A* and *B* correspond to the Cyt**1**·2PY Watson−Crick and sugar-edge isomers, respectively, as shown in Figure 3a and b. The selectivity of 266 nm ionization of these two Cyt**1**·2PY isomers is qualitatively consistent with the calculated ionization energies and relative abundances in the supersonic beam.

3.3. Electronic Excitation Energies. The vertical excitation energies and oscillator strengths for the Cyt·2PY and 1MCyt·2PY complexes were calculated at the CC2/aug-cc-pVDZ level using the MP2/aug-cc-pVTZ optimized ground-state geometries, and are presented in Table 2. The $S_1 \leftarrow S_0$ transitions are $^1\pi\pi^*$ excitations that are dominantly localized on the 2PY moiety. The CC2/aug-cc-pVDZ transition energies are generally about 15% higher than the experimental transition energies. The $S_1 \leftarrow S_0$ excitations of the Watson−Crick and sugar-edge isomers of Cyt**1**·2PY are calculated to be separated by ∼300 cm^{-1} with the Watson−Crick isomer at lower energy, close to the 1MCyt·2PY origin. This is in good correspondence with the observed spectra, where the transition of the Watson−Crick isomer appears at about 320 cm^{-1} lower energy than that of the sugar-edge isomer. This observation supports the above assignments. The adiabatic CC2/aug-cc-pVDZ $S_1 - S_0$ excitation energies of these three isomers are given in an additional table as Supporting Information: These energies confirm the UV-spectrum-based assignments performed in the present study. It is interesting to point out that the results of the CC2 calculations shown in Table 2 predict that the S_2 excited states lie 3000−6000 cm^{-1} above the S_1 states. Unfortunately, the calculated vertical excitation energies are not distinctive enough to assign the three minor isomers.

3.4. IR Depletion Spectra. *3.4.1. Isomer Identification and IR Spectra in the Hydride Stretching Region.* The IR/UV depletion spectra of the Cyt**1**·2PY WC and S isomers and of 1MCyt·2PY over the 2600−3800 cm^{-1} range are shown in Figure 7. All spectra show narrow bands of medium intensity

dx.doi.org/10.1021/jp409660b | J. Phys. Chem. B 2014, 118, 682−691

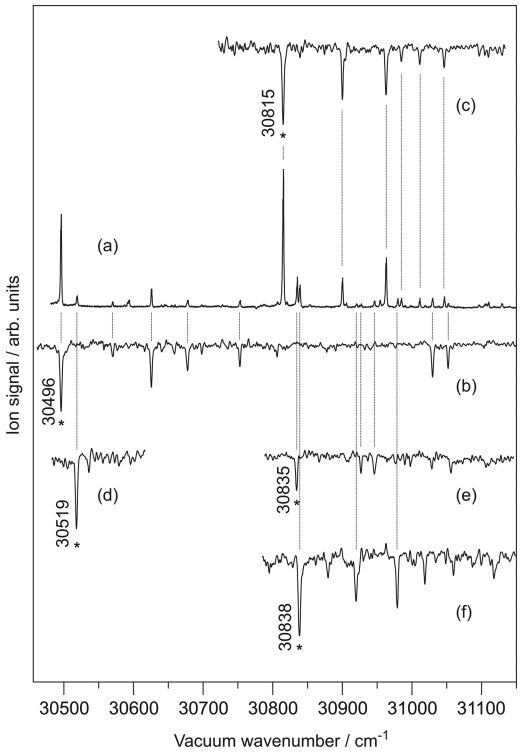

Figure 6. 2C-R2PI spectrum (a) measured in the cytosine·2-pyridone mass channel with laser ionization at 228 nm. Individual contributions to the R2PI spectrum identified by UV/UV depletion (b–f). The frequency of the detection laser for each spectrum is indicated by an asterisk.

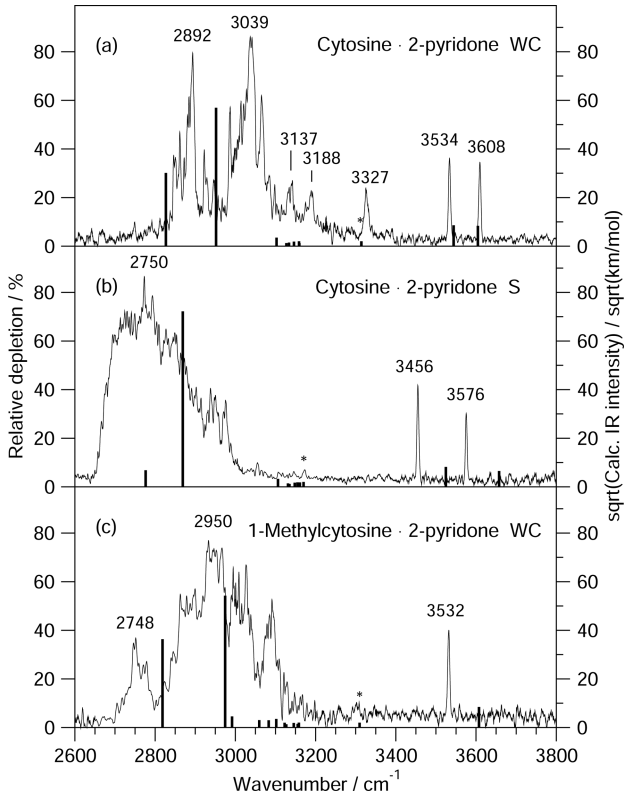

Figure 7. UV-detected IR depletion spectra of the cytosine·2-pyridone Watson–Crick (a) and sugar-edge (b) isomers and of 1-methylcytosine·2-pyridone (c). The relative depletion of the R2PI signal (in %) is indicated on the left scale. The PW91/6-311++G(d,p) calculated IR frequencies and intensities are indicated as stick plots, including the overtones of the NH_2-bend vibrations plotted with 10% of the fundamental intensity (marked by *). The square root of the intensity is plotted in order to make the weak bands clearly visible (right-hand scale).

between 3450 and 3610 cm^{-1} that correspond to free NH or $-NH_2$ stretch vibrations, and much broader and intense bands below 3200 cm^{-1} that arise from the H-bonded NH stretches. Weaker bands in the 3050–3150 cm^{-1} range are contributions from the CH stretches.

Due to N-methylation, the 1MCyt·2PY IR spectrum in Figure 7c must be that of the Watson–Crick dimer. The free NH stretch of the amino group gives rise to a narrow band at 3532 cm^{-1}. The strong antiparallel H-bonds lead to a shift of both the 2PY amide NH and cytosine amino NH stretch frequencies and a considerable intensity increase. This results in the intense and broad semistructured band in the 2700–3200 cm^{-1} region. In addition, the CH stretches borrow intensity from the intense NH band and also contribute to its shape.

The IR spectrum of Cyt**1**·2PY S is shown in Figure 7b. The two narrow bands at 3456 and 3576 cm^{-1} are due to the symmetric and antisymmetric NH_2 stretches. The spectrum is dominated by an intense, broad, and nearly structureless band between 2600 and 3100 cm^{-1}. This band is very similar to that observed in the IR spectrum of the 2PY self-dimer $(2PY)_2$, and corresponds to the strongly coupled NH stretch vibrations of the two H-bonded cis-amide groups.[37−39] The sugar-edge Cyt(**1**)·2PY complex is the only abundant isomer to exhibit antiparallel H-bonded amide groups, confirming the assignment of *B* as sugar-edge. We note that the broad band peaking at 2750 cm^{-1} is red-shifted compared to Cyt(**1**)·2PY WC in Figure 7a.

The IR spectrum of Cyt(**1**)·2PY WC is shown in Figure 7a. It is more structured with two clearly distinguishable bands around 2892 and 3039 cm^{-1}. We assign these as the H-bonded 2PY amide N1–H and cytosine-amino NH vibrations. The CH stretch vibrations give rise to lower-intensity bands at 3137 and 3188 cm^{-1}. The narrow bands at 3456 and 3576 cm^{-1} correspond to the free N1–H stretch and the free amino NH stretch of the cytosine moiety. We assign a narrow medium-intensity band at 3325 cm^{-1} to the first overtone of the NH_2 bend, in analogy to the amino bend overtones that appear in the IR spectra of the 2-aminopyridine·2PY[16] and $(2\text{-aminopyridine})_2$ dimers.[32]

Figure 7 also includes the PW91/6-311++G(d,p) calculated IR spectra of these three complexes as stickplots. In the analogous doubly H-bonded systems 2-aminopyridine·2PY and $(2\text{-aminopyridine})_2$, the PW91 calculated frequencies were also found to agree closely with the experimental IR frequencies.[16,32] The calculated IR spectrum of the Watson–Crick isomer of 1MCyt·2PY is in good agreement with the corresponding experimental spectrum in Figure 7c. For the spectra in Figure 7a and b, a good agreement is found with the Cyt(**1**)·2PY WC and S isomers. However, Table 5 shows that the agreement would also be good with the calculated spectra of the Cyt(**2b**)·2PY WC and S complexes. Comparison to the frequencies calculated with the correlated methods MP2/aug-cc-pVDZ and CC2/aug-cc-pVDZ did not yield additional clarification. Thus, because of the very similar IR frequencies of the Cyt(**1**)·2PY and Cyt(**2b**)·2PY complexes, the IR spectrum alone is not sufficient for an unambiguous identification of the observed isomers. Considering the thermodynamic and UV

dx.doi.org/10.1021/jp409660b | J. Phys. Chem. B 2014, 118, 682–691

Table 5. Calculated PW91/6-311++G(d,p) S_0 Vibrational Frequencies (in cm^{-1}) and Intensities (in km/mol) of the H-Bonded Complexes of 2-Pyridone with the Cytosine Tautomers 1, 2b, and 1-Methylcytosine in the Range of the Experimental IR Spectra

	Cyt**1**·2PY WC	Cyt**1**·2PY S	Cyt**2b**·2PY WC	Cyt**2b**·2PY S	1MCyt·2PY WC
mode	freq. (int.)	freq. (int.)	freq. (int.)	freq. (int.)	freq. (int.)
					1410.3 (25.8)
					1419.2 (9.9)
	1403.3 (58.3)	1436.9 (2.2)			1436.4 (9.4)
	1436.6 (12.0)	1452.6 (185.1)	1426.1 (168.1)	1435.7 (153.9)	1462.1 (3.5)
	1481.0 (5.2)	1477.2 (91.2)	1438.2 (6.5)	1444.0 (128.1)	1476.8 (18.7)
	1489.3 (177.9)	1484.9 (109.9)	1484.3 (5.3)	1493.1 (104.6)	1489.1 (143.1)
	1514.4 (150.8)	1538.6 (11.8)	1501.7 (61.4)	1506.2 (74.6)	1523.3 (182.9)
	1545.0 (111.0)	1551.6 (139.2)	1547.4 (166.3)	1541.8 (95.0)	1545.1 (106.9)
	1611.1 (9.7)	1585.1 (223.7)	1549.4 (57.4)	1550.3 (127.0)	1610.8 (23.7)
	1618.5 (153.9)	1615.3 (39.1)	1603.3 (258.6)	1588.3 (22.8)	1616.0 (140.7)
	1655.7 (301.4)	1635.8 (714.9)	1618.1 (161.6)	1611.5 (840.8)	1654.9 (283.1)
	1668.8 (240.3)	1666.4 (270.6)	1651.4 (315.8)	1617.6 (155.8)	1661.1 (159.5)
	1711.5 (834.5)	1672.3 (1252.5)	1677.8 (550.3)	1685.9 (554.6)	1698.8 (875.4)
NH_b (OH_b) str. s	2826.8 (907.0)	2776.4 (46.8)	2926.6 (933.7)	2687.2 (262.2)	2818.5 (1321.1)
NH_b (OH_b) str. as	2952.0 (3242.7)	2868.9 (5211.0)	3043.5 (2803.5)	2807.0 (5738.7)	2974.5 (2940.3)
1MCyt methyl CH str.					2991.7 (21.1)
1MCyt methyl CH str.					3059.7 (9.3)
1MCyt methyl CH str.					3083.1 (9.1)
Cyt CH stretch	3133.9 (2.2)	3131.2 (2.0)	3097.3 (6.5)	3081.9 (24.6)	3122.9 (3.9)
	3159.6 (1.6)	3154.7 (3.5)	3138.6 (6.6)	3139.1 (7.3)	3155.5 (2.3)
2PY CH stretches	3102.6 (12.5)	3106.2 (10.8)	3104.8 (7.4)	3108.5 (9.4)	3102.0 (12.4)
	3127.3 (1.6)	3134.9 (1.4)	3133.2 (0.5)	3127.6 (5.2)	3126.9 (1.8)
	3146.2 (3.5)	3148.1 (2.9)	3147.6 (2.6)	3150.3 (2.0)	3145.6 (3.6)
	3158.8 (4.1)	3160.9 (3.3)	3160.3 (3.2)	3160.3 (3.5)	3158.3 (4.1)
Cyt amide NH_f str.	3544.0 (73.9)				
Cyt amino NH_f str.	3604.5 (70.1)		3611.4(74.0)		3674.7 (71.5)
Cyt NH_2 str.(s)		3524.7 (67.3)		3523.2 (64.7)	
Cyt NH_2 str.(as)		3657.6 (42.7)		3654.0 (40.8)	
Cyt OH_f str.			3667.2 (85.8)		

spectroscopic results discussed above, we assign the experimental IR spectrum in Figure 7a to the Cyt**1**·2PY Watson−Crick and Figure 7b to the Cyt**1**·2PY sugar-edge complex, supporting the assignment of the UV spectra.

3.4.2. Comparison to Other Watson−Crick H-Bonded Dimers. Recently, Nosenko et al.[26] have measured the IR depletion spectra of the jet-cooled dimers 4-aminopyrimidine·1-methylthymine (4APM·1MT) and 4-aminopyrimidine·6-methyl-4-pyrimidinone (4AP·M4PMN), and have compared them to the IR spectrum of 2-aminopyridine·2-pyridone (2AP·2PY).[16] All three dimers mimic the Watson−Crick hydrogen bond pattern of adenine:uracil or adenine:thymine. The free amino NH stretch vibrations in these three dimers are found in the narrow range between 3530 and 3538 cm^{-1}, and the overtones of the amino NH_2 bend mode lie between 3299 and 3323 cm^{-1}. This vibrational pattern is well reproduced by the two Watson−Crick dimers Cyt**1**·2PY WC and 1MCyt·2PY WC studied here, with N−H stretch frequencies at 3534 and 3532 cm^{-1}, respectively, and the Cyt**1**·2PY WC NH_2 bend overtone at 3327 cm^{-1}. The NH_2 bend overtone of 1MCyt·2PY WC is tentatively assigned to the very weak feature at ∼3300 cm^{-1}.

Nosenko et al.[26] have reported the H-bonded amino-NH stretch vibrations at 3205 and 3130 cm^{-1} for 4APM·1MT and for 4APM·M4PMN, respectively. These bands are shifted by −360 and −435 cm^{-1} with respect to the antisymmetric NH_2 stretch vibration of the 4APM monomer. The corresponding H-bonded amino-NH stretch shifts in this work are about −600 cm^{-1}. This more pronounced shift reflects the stronger hydrogen-bonding interaction of the Watson−Crick dimers Cyt**1**·2PY and 1MCyt·2PY. The calculated dissociation energies of about 21 kcal/mol are roughly twice as large as those reported for 4APM·1MT and 4APM·M4PMN.[26]

3.4.3. IR Depletion Spectra and Vibrations in the Carbonyl Stretching Region. The IR/UV depletion spectra in the 1400−2000 cm^{-1} range are presented in Figure 8. The PW91/6-311++G(d,p) calculated IR spectra are indicated as stick-plots below the measured spectra. The 1MCyt·2PY spectrum in Figure 8c shows two bands at 1670 and 1702 cm^{-1} that we assign to the hydrogen-bonded C═O stretch of the 2PY moiety and to the free C═O stretch of the 1MCyt moiety, respectively. The Cyt·2PY WC spectrum in Figure 8a exhibits a very similar band structure with two intense bands at 1663 and 1694 cm^{-1}, assigned to the C═O stretching vibration of 2PY (H-bonded) and Cyt (free).

A more structured and bathochromically shifted band pattern is observed for the Cyt·2PY S isomer, shown in Figure 8b. This indicates that the interaction between the monomers is clearly different and somewhat stronger than that in the Cyt·2PY and 1MCyt·2PY Watson−Crick isomers, as seen in Figure 8a and c, which is consistent with the assignment to the sugar-edge **1**·2PY complex.

However, we note that the IR spectra of the different Cyt·2PY complexes in the carbonyl stretch range are not as specific as one might expect. From calculated normal modes and IR

dx.doi.org/10.1021/jp409660b | J. Phys. Chem. B 2014, 118, 682−691

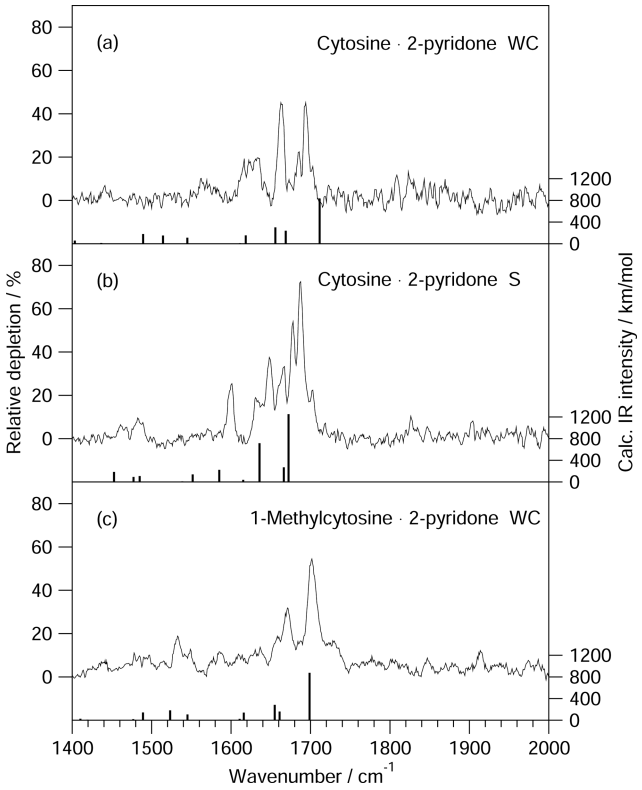

Figure 8. IR/UV depletion spectra of the cytosine·2-pyridone Watson–Crick (a) and sugar-edge (b) complexes and of the 1-methylcytosine·2-pyridone complex in the C=O stretch range. The PW91/6-311++G(d,p) calculated IR spectra are indicated as stick plots.

intensities in Table 5, it is even hardly possible to distinguish between the complexes containing the amino-keto and amino-hydroxy tautomers of cytosine.

4. CONCLUSIONS

The doubly hydrogen-bonding complexes of cytosine and of 1-methylcytosine with 2-pyridone were probed using mass- and isomer-specific UV and infrared spectroscopic techniques. Five different isomers of cytosine·2-pyridone were observed in the molecular jet.

The two most abundant of these were clearly identified as the complexes of keto-amino cytosine **1** with 2-pyridone bound through its Watson–Crick (*A*) and sugar-edge (*B*) binding sites. The assignments rest on (a) ab initio gas-phase thermodynamic calculations of isomer abundances, (b) UV/UV hole-burning experiments at two different ionization energies (266 and 228 nm), (c) two-color R2PI spectra of the 50–200 cm^{-1} intermolecular vibrational stretching region, (d) species-specific IR depletion spectra in the intramolecular NH and CO stretching regions, and (e) comparisons of calculated UV excitation energies and (f) calculated ionization energies. Our assignments are supported by every one of these methods or properties.

A further strong support of the assignment of isomer *A* as the Watson–Crick form is based on the comparison to the UV and IR depletion spectra of 1-methylcytosine·2-pyridone. This dimer can only exist in one H-bonded isomeric form bound through the Watson–Crick binding site. While the combination of the applied techniques allows an unambiguous identification of the different complexes observed, it is important to note that assignments based on only one of them are usually not conclusive.

The binding energies calculated for the Cyt·2PY Watson–Crick and sugar-edge complexes and for the 1MCyt·2PY complex are close to −22 kcal/mol; see Table 1. Thus, the complexes formed by the cytosine and 1-methylcytosine keto-amino tautomer are bound significantly stronger than those formed by all other cytosine tautomers, as shown in this work. More generally, the cytosine·2-pyridone complexes are among the most stable doubly H-bonded dimers.[40] The only exceptions in the JSCH-2005 database of Hobza and co-workers that we could find are the inosine···cytosine and guanine···guanine base pairs, with calculated binding energies of −24.2 and −22.7 kcal/mol, respectively.[40] The calculated binding energies of the other doubly H-bonded nucleobase complexes are typically smaller than −20 kcal/mol.[40]

As a direct experimental measure for the H-bond interaction strength, we have determined the harmonic force constants for the S_1 state H-bond stretching vibration σ' in the pseudodiatomic approximation. For the Cyt·2PY sugar-edge, Watson–Crick, and 1MCyt·2-PY complexes, these force constants are 67, 51, and 55 N/m, respectively. Compared to force constants for single hydrogen bonds, which range from ∼2 to 25 N/m,[41] the obtained values indicate a very strong interaction, even for a doubly hydrogen-bonded system.

■ ASSOCIATED CONTENT

Ⓢ Supporting Information

A table of CC2 vertical and adiabatic excitation energies of cytosine **1**·2-pyridone (Watson–Crick), cytosine **1**·2-pyridone (sugar-edge), and 1-methyl-cytosine **1**·2-pyridone and three tables with the corresponding MP2/aug-cc-pVTZ optimized ground-state structures. This material is available free of charge via the Internet at http://pubs.acs.org.

■ AUTHOR INFORMATION

Corresponding Author

*E-mail: leutwyler@dcb.unibe.ch.

Notes

The authors declare no competing financial interest.

■ ACKNOWLEDGMENTS

Financial support by the Schweiz. Nationalfonds (project no. 200020-132540) is gratefully acknowledged.

■ REFERENCES

(1) Dreyfus, M.; Bensaude, O.; Dodin, G.; Dubois, J. E. Tautomerism in Cytosine and 3-Methylcytosine. A Thermodynamic and Kinetic Study. *J. Am. Chem. Soc.* **1976**, *98*, 6338–6349.

(2) Szczesniak, M.; Szczepaniak, K.; Kwiatkowski, J. S.; Kubulat, K.; Person, W. B. Matrix Isolation Infrared Studies of Nucleic Acid Constituents. 5. Experimental Matrix-Isolation and Theoretical ab Initio SCF Molecular Orbital Studies of the Infrared Spectra of Cytosine Monomers. *J. Am. Chem. Soc.* **1988**, *110*, 8319–8330.

(3) Bazso, G.; Tarczay, G.; Fogarasi, G.; Szalay, P. G. Tautomers of Cytosine and their Excited Electronic States: A Matrix Isolation Spectroscopic and Quantum Chemical Study. *Phys. Chem. Chem. Phys.* **2011**, *13*, 6799–6807.

(4) Brown, R. D.; Godfrey, P. D.; McNaughton, D.; Pierlot, A. P. Tautomers of Cytosine by Microwave Spectroscopy. *J. Am. Chem. Soc.* **1989**, *111*, 2308–2310.

(5) Alonso, J. L.; Vaquero, V.; Peña, I.; López, J. C.; Mata, S.; Caminati, W. All Five Forms of Cytosine Revealed in the Gas Phase. *Angew. Chem., Int. Ed.* **2013**, *52*, 2331–2334.

(6) Feyer, V.; Plekan, O.; Richter, R.; Coreno, M.; Vall-Ilosera, B.; Prince, K. C.; Trofimov, A. B.; Zaytseva, I. L.; Moskovskaya, T. E.; Gromov, E. V.; et al. Tautomerism in Cytosine and Uracil: An Experimental and Theoretical Core Level Spectroscopic Study. *J. Phys. Chem. A* **2009**, *113*, 5736−5742.
(7) Feyer, V.; Plekan, O.; Kivimäki, A.; Prince, K. C.; Moskovskaya, T. E.; Zaytseva, I. L.; Soshnikov, D. Y.; Trofimov, A. B. Comprehensive Core-Level Study of the Effects of Isomerism, Halogenation, and Methylation on the Tautomeric Equilibrium of Cytosine. *J. Phys. Chem. A* **2011**, *115*, 7722−7733.
(8) Kostko, O.; Bravaya, K.; Krylov, A.; Ahmed, M. Ionization of Cytosine Monomer and Dimer Studied by VUV Photoionization and Electronic Structure Calculations. *Phys. Chem. Chem. Phys.* **2010**, *12*, 2860−2872.
(9) Nir, E.; Müller, M.; Grace, L. I.; de Vries, M. REMPI Spectroscopy of Cytosine. *Chem. Phys. Lett.* **2002**, *355*, 59−64.
(10) Nir, E.; Hünig, I.; Kleinermanns, K.; de Vries, M. S. The Nucleobase Cytosine and the Cytosine Dimer Investigated by Double-Resonance Laser Spectroscopy and Ab Initio Calculations. *Phys. Chem. Chem. Phys.* **2003**, *5*, 4780−4785.
(11) Lobsiger, S.; Leutwyler, S. The Adiabatic Ionization Energy and Triplet T_1 Energy of Jet-Cooled Keto-Amino Cytosine. *J. Phys. Chem. Lett.* **2012**, *3*, 3576−3580.
(12) Lobsiger, S.; Trachsel, M. A.; Frey, H. M.; Leutwyler, S. Excited-State Dynamics of Cytosine: The Decay of the Keto-Amino Tautomer is Not Ultrafast. *J. Phys. Chem. B* **2013**, *117*, 6106−6115.
(13) Morpurgo, S.; Bossa, M.; Morpurgo, G. O. Ab Initio Study of Intramolecular Proton Transfer Reactions in Cytosine. *Chem. Phys. Lett.* **1997**, *280*, 233−238.
(14) Trygubenko, S. A.; Bogdan, T. V.; Rueda, M.; Orozco, M.; Luque, F. J.; Sponer, J.; Slavicek, P.; Hobza, P. Correlated Ab Initio Study of Cytosine and its Tautomers in the Gas Phase, in a Microhydrated Environment and in Aqueous Solution. *Phys. Chem. Chem. Phys.* **2002**, *4*, 4192−4203.
(15) Held, A.; Champagne, B. B.; Pratt, D. Inertial Axis Reorientation in the $S_1 \leftarrow S_0$ Electronic Transition of 2-Pyridone - A Rotational Duschinsky Effect - Structural and Dynamic Consequences. *J. Chem. Phys.* **1991**, *95*, 8732−8743.
(16) Frey, J. A.; Müller, A.; Frey, H.-M.; Leutwyler, S. Infrared Depletion Spectra of 2-Aminopyridine-2-Pyridone, a Watson-Crick Mimic of Adenine-Uracil. *J. Chem. Phys.* **2004**, *121*, 8237−8245.
(17) Leist, R.; Frey, J. A.; Leutwyler, S. Fluorobenzene−Nucleobase Interactions: Hydrogen Bonding or π-Stacking? *J. Phys. Chem. A* **2006**, *110*, 4180−4187.
(18) Müller, A.; Leutwyler, S. The Nucleobase Pair Analogues 2-Pyridone·Uracil, 2-Pyridone·Thymine and 2-Pyridone·5-Fluorouracil: Hydrogen Bond Strengths and Intermolecular Vibrations. *J. Phys. Chem. A* **2004**, *108*, 6156−6164.
(19) Müller, A.; Frey, J. A.; Leutwyler, S. Probing the Watson-Crick, Wobble and Sugar-Edge Hydrogen Bond Sites of Uracil and Thymine. *J. Phys. Chem. A* **2005**, *109*, 5055−5063.
(20) Frey, J. A.; Leist, R.; Müller, A.; Leutwyler, S. Gas-Phase Watson-Crick and Hoogsteen Isomers of the Nucleobase Mimic 9-Methyladenine·2-Pyridone. *ChemPhysChem* **2006**, *7*, 1494−1499.
(21) Holbrook, S. R.; Cheong, C.; Tinoco, I.; Kim, S.-H. Crystal Structure of an RNA Double Helix Incorporating a Track of non-Watson-Crick Base Pairs. *Nature* **1991**, *353*, 579−581.
(22) Limmer, S. In *Mismatch Base Pairs in {RNA}*; Moldave, K., Ed.; Progress in Nucleic Acid Research and Molecular Biology; Academic Press: San Diego, CA, 1997; Vol. *57*, pp 1−39.
(23) Nir, E.; Plützer, C.; Kleinermanns, K.; de Vries, M. S. Properties of Isolated DNA Bases, Base Pairs and Nucleosides Examined by Laser Spectroscopy. *Eur. Phys. J. D* **2002**, *20*, 317−329.
(24) Nir, E.; Janzen, C.; Imhof, P.; Kleinermanns, K.; de Vries, M. S. Pairing of the Nucleobases Guanine and Cytosine in the Gas Phase Studied by IR-UV Double-Resonance Spectroscopy and Ab Initio Calculations. *Phys. Chem. Chem. Phys.* **2002**, *4*, 732−739.
(25) Abo-Riziq, A.; Grace, L.; Nir, E.; Kabelač, M.; Hobza, P.; de Vries, M. S. Photochemical Selectivity in Guanine-Cytosine Base-Pair Structures. *Proc. Natl. Acad. Sci. U.S.A.* **2005**, *102*, 20−23.
(26) Nosenko, Y.; Kunitski, M.; Stark, T.; Gobel, M.; Tarakeshwar, P.; Brutschy, B. Vibrational Signatures of Watson-Crick base Pairing in Adenine-Thymine Mimics. *Phys. Chem. Chem. Phys.* **2013**, *15*, 11520−11530.
(27) Trofimov, A. B.; Schirmer, J.; Kobychev, V. B.; Potts, A. W.; Holland, D. M. P.; Karlsson, L. Photoelectron Spectra of the Nucleobases Cytosine, Thymine and Adenine. *J. Phys. B: At., Mol. Opt. Phys.* **2006**, *39*, 305−329.
(28) Bosenberg, W.; Guyer, D. Single-Frequency Optical Parametric Oscillator. *Appl. Phys. Lett.* **1992**, *61*, 387−389.
(29) Peterson, K. A.; Woon, D. E.; T. H. Dunning, J. Benchmark Calculations with Correlated Molecular Wave Functions. IV. The Classical Barrier Height of the $H+H_2 \rightarrow H_2+H$ Reaction. *J. Chem. Phys.* **1994**, *100*, 7410−7415.
(30) Bachorz, R. A.; Bischoff, F. A.; Höfener, S.; Klopper, W.; Ottiger, P.; Leist, R.; Frey, J. A.; Leutwyler, S. Scope and Limitations of the SCS-MP2Method for Stacking and Hydrogen Bonding Interactions. *Phys. Chem. Chem. Phys.* **2008**, *10*, 2758−2766.
(31) TURBOMOLE *V6.3 2011*; A Development of Universität Karlsruhe (TH) and Forschungszentrum Karlsruhe GmbH, 1989−2007, TURBOMOLE GmbH; available from http://www.turbomole.com.
(32) Ottiger, P.; Frey, J. A.; Frey, H.-M.; Leutwyler, S. Jet-Cooled 2-Aminopyridine Dimer: Conformers and Infrared Vibrational Spectra. *J. Phys. Chem. A* **2009**, *113*, 5280−5288.
(33) Frisch, M. J.; Trucks, G. W.; Schlegel, H. B.; Scuseria, G. E.; Robb, M. A.; Cheeseman, J. R.; Scalmani, G.; Barone, V.; Mennucci, B.; Petersson, G. A.; et al. *Gaussian 03*, revision B.03; Gaussian, Inc.: Wallingford, CT, 2004.
(34) Frey, J. A.; Leist, R.; Tanner, C.; Frey, H. M.; Leutwyler, S. 2-Pyridone: The Role of Out-of-Plane Vibrations on the $S_1 \leftrightarrow S_0$ Spectra and S_1 State Reactivity. *J. Chem. Phys.* **2006**, *125*, 114308−114321.
(35) Müller, A.; Talbot, F.; Leutwyler, S. Intermolecular Vibrations of the Jet Cooled 2PY-2HP Mixed Dimer, a Model for Tautomeric Nucleic Acid Base Pairs. *J. Chem. Phys.* **2001**, *115*, 5192−5202.
(36) Müller, A.; Talbot, F.; Leutwyler, S. Hydrogen-Bond Vibrations of 2-Aminopyridine-2-Pyridone, a Watson-Crick Analogue of Adenine-Uracil. *J. Am. Chem. Soc.* **2002**, *124*, 14486−14494.
(37) Matsuda, Y.; Ebata, T.; Mikami, N. Population Labeling Spectroscopy for the Electronic and the Vibrational Transitions of 2-Pyridone and its Hydrogen-Bonded Clusters. *J. Chem. Phys.* **2000**, *113*, 573−580.
(38) Matsuda, Y.; Ebata, T.; Mikami, N. IR-UV Double Resonance Spectroscopic Study of 2-Hydroxypyridine and its Hydrogen-Bonded Clusters. *J. Phys. Chem. A* **2001**, *105*, 3475−3480.
(39) Borst, D. R.; Roscioli, J. R.; Pratt, D. W.; Florio, G. M.; Zwier, T. S.; Müller, A.; Leutwyler, S. Hydrogen Bonding and Tunneling in the 2-Pyridone·2-Hydroxypyridine Dimer. Effect of Electronic Excitation. *Chem. Phys.* **2002**, *283*, 341−354.
(40) Jurečka, P.; Šponer, J.; Černy, J.; Hobza, P. Benchmark Database of Accurate (MP2 and CCSD(T) Complete Basis Set Limit) Interaction Energies of Small Model Complexes, DNA Base Pairs and Amino Acid Pairs. *Phys. Chem. Chem. Phys.* **2006**, *8*, 1985−1993.
(41) Legon, A. C.; Millen, D. J. Gas-Phase Spectroscopy and the Properties of Hydrogen-Bonded Dimers:HCN-HF as the Spectroscopic Prototype. *Chem. Rev.* **1986**, *86*, 635−657.